**International Journal of Mining Science (IJMS)**
*Volume 4, Issue 4, 2018, PP 10-24*
*ISSN 2454-9460 (Online)*
*DOI: http://dx.doi.org/10.20431/2454-9460.0404002*
*www.arcjournals.org*

# Trace and Rare Earth Elements Patterns in Metamorphosed Ultramafic Rocks of the Paleoproterozoic Nyong Series, Southeast Cameroon

**T. A. Ako [1, 2*], A. Vishiti[3], C. E. Suh[2], A. C. Kedia[2], O. Omang[1, 4]**

[1]*Department of Geology, Federal University of Technology, Minna, Nigeria.*

[2] *Department of Geology, University of Buea, Cameroon.*

[3]*Department of Mining and Extractive Metallurgy, Institute of Science, Engineering and Technology, Cameroon Christian University, Bali, Cameroon.*

[4] *Department of Mineral and Petroleum Resources Engineering, Federal Polytechnic, Auchi, Nigeria.*

***Corresponding Author:** ***T. A. Ako,*** *Department of Geology, Federal University of Technology, Minna, Nigeria, Department of Geology, University of Buea, Cameroon.*

**Abstract:** *Meta-ultramafic rocks from the Paleoproterozoic Nyong Series (SE Cameroon) were investigated in this study. The aim was to study trace and rare earth elements (REEs) patterns in these rocks. A layered sequence exposed on a cliff face was mapped. Samples from the various horizons were collected and subsequently analysed in the laboratory for their petro graphic and whole rock chemical compositions (but only the results of trace and rare earth elements are presented in this study). All the samples from the study area define a light trend on a (Nb/Th) vs (Th/Yb) plot, and have low ( Nb/Th) average ratio of 0.6 and elevated (Th/Yb) average ratio of 1.0 These two characteristics, i.e. ( Nb/Th) < 1 and (Th/Yb) >1, are generally accepted to be the product of crustal contamination of mantle-derived magmas. Relative to the primitive mantle, the rocks show relative enrichment of LILEs (such as Sc, Rb, Ba, Th and U) with very steep slopes and depletion of HFSE (such as Ta and Nb) which also show very steep and gentle slopes respectively. They are further characterized by distinct troughs such as Ta-Nb and Sr-Nb. These features are characteristics of tholeiitic basalts produced at destructive plate margins or within plate tholeiites contaminated by continental crust. The samples are enriched in LREEs (LREE/HREE >1). Average Eu* and Ce* values in the samples are 0.72 and 1.87 respectively while average $La/Yb_N$ is 0.79. Primitive mantle normalised REE plots of the ultramafic rocks are characterized by four distinct types of patterns based on their shapes and Eu anomalies (Eu*). Type 1 samples are characterised by steep LREE patterns, slightly positive Eu* and flat HREE patterns. Type 2 exhibit LREE patterns with high peak values for La and Pr, V-shape Ce anomaly, a very gentle HREE pattern and a moderate negative Eu*. Type 3 samples show a steep LREE patterns, strong negative Eu* and flat HREE patterns whereas Type 4 samples display flat and very steep LREE patterns, a very strong negative Eu* and a very flat HREE patterns. Generally, all the four types are characterized by enrichment in LREEs and depletion in HREEs and a negative Eu and Ce anomalies except the type 1. Negative Eu anomaly are all features that suggest removal of plagioclase component from the basic magma or may be due to the magma that might segregated at depth where plagioclase is not stable and thus could not have fractionated.*

**Keywords:** *Rare earth elements, enrichment in LILE, depleted in HFSE, HREE and LREE patterns, Eu anomalies (Eu*) and primitive mantle.*

## 1. INTRODUCTION

Trace elements are elements with very low concentration in rocks and consequently they do not normally appear in the chemical formulae of major rock forming minerals. The concentration of trace elements is usually expressed in parts per million (ppm) or in rare instances in parts per billion (ppb) and they have wide application in geochemistry, petrology and mineral exploration. They can be used to trace the origin of rocks, their tectonic settings, evolution and alteration, and in finger-printing ore deposits (Hugh, 1993; Randine *et al*., 2014 and Randine *et al*., 2015). Similar to the trace elements, are the rare earth elements (REEs) which are a special group of trace elements and are divided into two groups. These are the heavy rare earth elements (HREEs) which have high atomic number and the

light rare earth elements (LREEs) which have low atomic number. They are the most useful of all trace elements and have important application in the study of igneous, metamorphic and sedimentary rocks (Ranvine *et al*., 2014).

The Rare Earth Elements (REE), commonly known as lanthanides, having atomic numbers ranging from Lanthanum (La) 57 to Lutetium (Lu) 71. The lanthanides have very similar geochemical properties because they occur in 3+ ionic forms in nature. However, Europium (Eu) also occur in 2+ (larger ion) and Cerium (Ce) in 4+ (smaller ion) oxidation states. They only differ in number of electrons in the 4f shell; this shell has no involvement in forming chemical bonds, therefore the elements have very similar chemical properties. The major difference amongst REEs is their size, which decreases with increasing atomic number. This variation is due to the increased nuclear charge, which is only partially shielded by the 4f electrons; this feature is also known as 'lanthanide contraction'. Due to size differences, REEs can preferentially substitute in different minerals. Though such difference is small, it has a significant bearing on partitioning of REEs in different minerals (Henderson, 1984; Boynton, 1989; Rollinson, 1993; Randive, 2012). This slight difference has been exploited by a number of petro logical processes causing the REEs to become fractionated relative to each other. It is this phenomenon which is used by geochemistry to probe into genesis of rocks and uncover the petro logical processes involved in their formation. Rare earth elements have a range of implications in petrology: (1) in magmatic systems, REEs can provide an indication of the nature of the source region of the magmas, e.g. magma derived from the melting of peridotitic mantle have different REEs patterns from magmas derived from garnet-bearing portions of the mantle and they also give an indication of the mineralogical composition of the residue in the mantle, and (2) Degree of differentiation. Certain minerals can easily incorporate certain REEs into their structure, e. g. plagioclase feldspar easily incorporate Eu into its crystal lattice. Therefore, the crystallization of plagioclase from magma will progressively deplete the melt of Eu (Hugh, 1993; Ding *et al*., 2012; Dare *et al*., 2014 and Barnes *et al*., 2015**).**

In order to interpret trace and REEs data, it is usually required the data be normalized and the result of such normalization is known as trace and REEs patterns with the y-axis on a log scale. Normalization requires that the concentration of the element in the rock be divided by the concentration of the corresponding element in a reference standard. In petrology, these standards include the primitive mantle and the $C_1$ chondrite. However, the Post Achaean Australian Shield (PAAS) as well as the North Atlantic Shale Composite (NASC) are also used especially for metasedimentary rocks (Sun *et al*., 1979; Taylor and McLennan, 1985; Hofmann, 1988 and Verhulst *et al*., 2000).

The REE content of metamorphic rocks is assumed to be similar to that of their protolith. However, it is observed that under some circumstances the REEs are mobile, whereas, in other circumstances they are immobile. Thus the overall REE abundance of metamorphic rocks may differ considerably from their protoliths. The residence of REEs in metamorphic rocks depends on the minerals present in that rock. Therefore, the modal abundance of those minerals and the physical and chemical conditions in which those minerals grew (assuming that the minerals were not subsequently altered) pose strong constraint on REEs distribution in metamorphic rocks (Ranvine *et al*., 2014). The changes in mineral assemblages and mineral composition have been extensively documented for a wide variety of metamorphic terranes (e.g. Winkler, 1976; Miyashiro, 1973 and Ferry, 1982). It is observed that the accessory minerals (zircon, monazite, xenotime, allanite, sphene and apatite) tend to concentrated REE much more than do the major rock forming minerals such as feldspars, micas, pyroxenes and amphiboles. Quartz has a very low REE content. The REE concentration of individual minerals and partitioning of REEs between minerals are controlled by the P-T-X condition in which the minerals form and a variety of crystallo-chemical factors, such as valence and effective ionic radius (Fleischer and Alteschuler, 1969; Jensen, 1973; Reitan *et al*., 1980 and Henderson, 1984). Petrologic data describing the reactions (both continuous and discontinuous) that occurred during metamorphism should be especially useful in determining reasonable constraints. For example, if garnets were to disappear, the REE (especially HREE) released would have to leave the system or to be incorporated in other phases. Such reactions should be studied in detail to estimate overall influence of metamorphism on REE distribution (Ranvine *et al*., 2014).

This paper focuses on the metamorphosed ultramafic intrusions belonging to the Paleoproterozoic Nyong Series in SE Cameroon. Geochemical data of the rocks are presented in order to depict their

trace and REEs patterns and provide valuable information on their mantle source region (degree of partial melting, fractionation, heterogeneity assimilation or contamination and metasomatism). Petro logical, mineralogical and other geochemical data (major oxides, Ni-Cu-PGEs) of the rocks have already been presented by Ako *et al*., 2015; Ako, 2016; Ako *et al*., 2017a and Ako *et al*., 2017b) and are not discussed any further.

## 2. REGIONAL GELOGICAL SETTING

The Nyong Series lies within the West Central African Belt (WCAB) (Figure 1) which is a N-S-trending Paleoproterozoic belt that extends along the western side of the Congo craton from Angola to Cameroon (Feybesse *et al.,* 1998), and continues to NE Brazil as the Transamazonia belt (Penaye *et al.*, 2004; Lerouge *et al.*, 2006; Owona, 2008; Owona *et al*., 2011 and Owona *et al*., 2013). The WCAB includes the Nyong complex in Cameroon known as the lower Nyong Unit (Maurizot *et al.*, 1986); the Franceville-Ogoue complex in Gabon and the West Congolese complex in the Republic of Congo and Democratic Republic of Congo (Bonhomme *et al.*, 1982; Feybesse *et al*., 1998; Vitcat and Pouclet, 2000; Tack *et al.*, 2001).

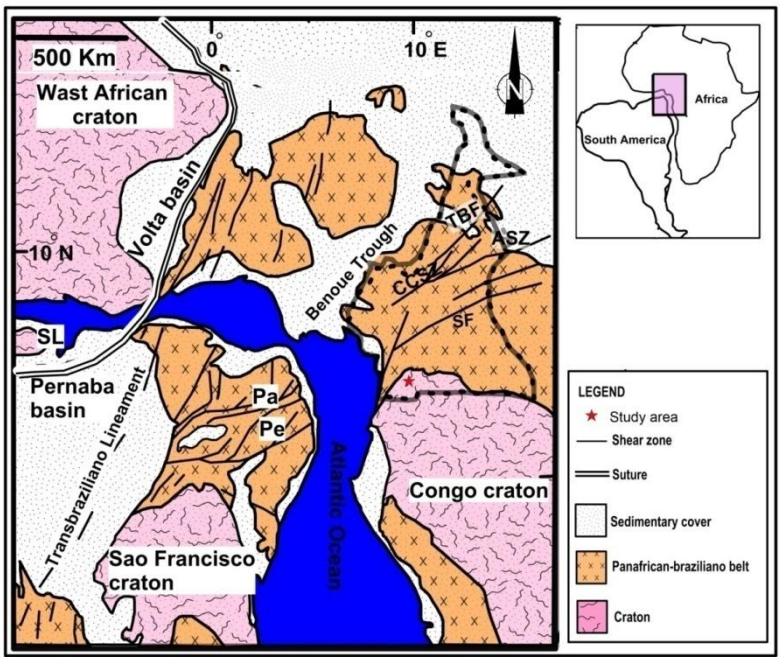


**Figure1.** *Geological map of the pre-drift Gondwana showing the Congo craton in Cameroon and the northern part of São Francisco craton of Brazil (modified after Ebah Abeng et al., 2012).*

This large belt resulted from the collision between the Congo and São Francisco cratons. Most of the WCAB is characterized by tectonic reworking of Achaean crust with little addition of juvenile material, particularly in the southern part of the belt (Thomas *et al.,* 2002; Toteu *et al.,* 1994a). However, this dominant recycling character is diminished northward with the appearance of ~ 2.1 Ga juvenile metasedimentary and meta-plutonic rocks intensively reworked and dismembered in the Pan-African belt north of the Congo craton (Pénaye *et al.,* 2004). The Nyong Series (coined as Nyong Group, e.g. Lerouge *et al.*, 2006; Owona, 2008; Owona *et al.*, 2011; Owona *et al*., 2013) in the northwestern corner of the Congo craton in Cameroon is a-well-preserved granulitic unit of the WCAB resting as an Eburnean nappe on the Congo craton (Feybesse *et al.*, 1986; Toteu *et al.*, 1994b). The high-grade metamorphism associated with arrested charnockite formation in this unit is dated at 2050 Ma (Toteu *et al.*, 1994b); Lerouge *et al.*, 2006). However, it is not clear whether or not these Paleoproterozoic tectono-metamorphic events were accompanied by any sedimentation or magmatism. This led to the assertion thatthe Nyong Series is a reworked part of the Congo craton in Cameroon (Lasserre and Soba, 1976; Faybesse *et al.*, 1986; Owona, 2008, Owona *et al*., 2011; Owona *et al*., 2013). Within the Cameroon context the series has been called the Nyong Unit by some authors (e.g. Ebah Abeng *et al.*, 2012). The Nyong Unit is bordered by the Ntem Unit in the SE, the Pan-African gneiss to the north and NE and by the Quaternary sedimentary formations (Kribi Campo basin) at the NW parts (Figure 2).

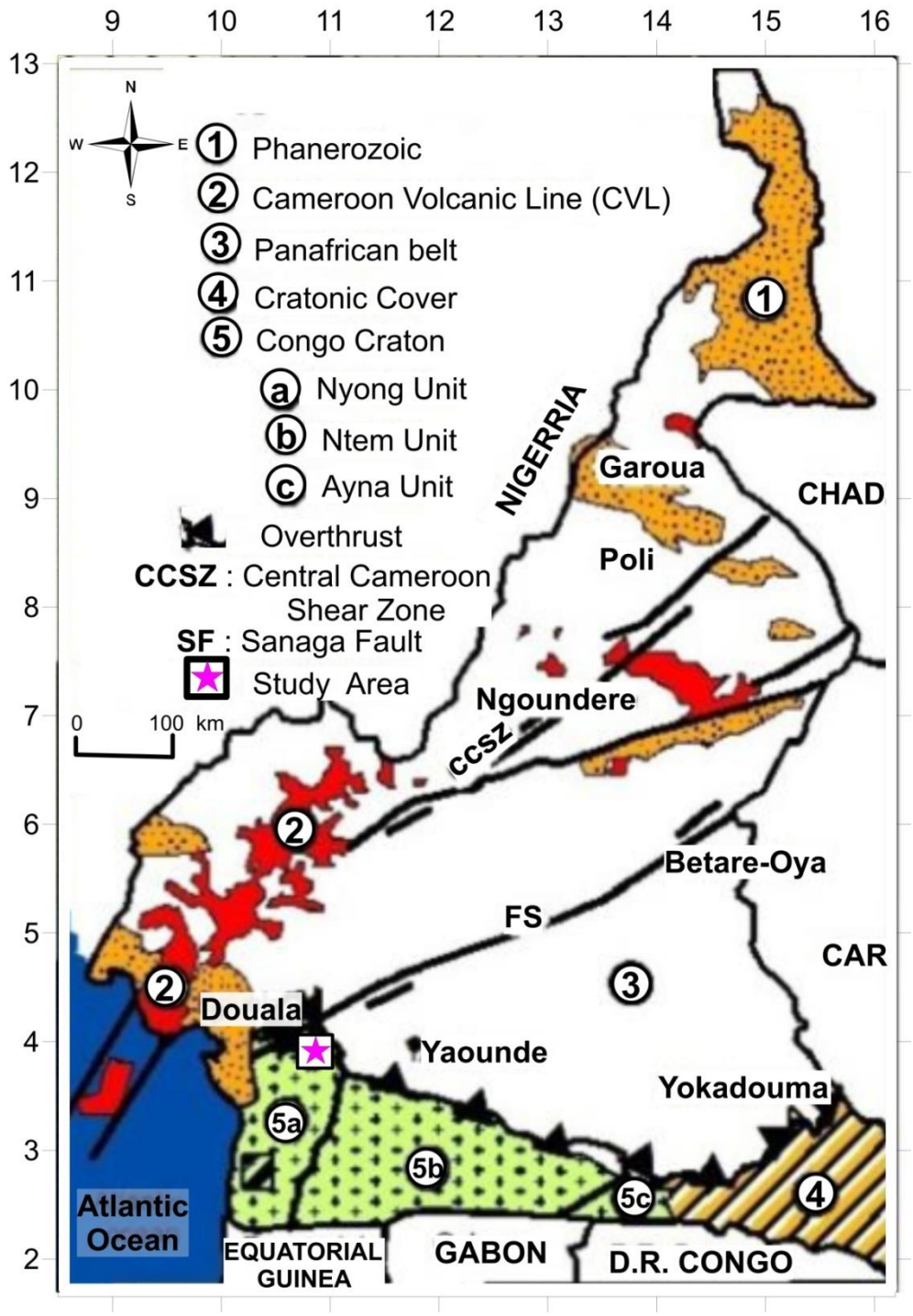


**Figure2.** *Geological map of Cameroon showing the relationship between the Nyong Unit (study area), Ntem Unit, Pan-African gnesises and the Quaternary sedimentary formations (modified after Ebah Abeng et al., 2012).*

It is a high grade-gneiss unit, which was initially defined as a Neoproterozoic, or a Palaeoproterozoic reactivated NW corner of the Archaean Congo Craton (Lasserre and Soba, 1976; Feybesse *et al*., 1986, Lerouge *et al.*, 2006). The Nyong Unit is made up of a greenstone belt (pyroxenites, amphibolo-pyroxenites, peridotites, talcschists, amphibolites and banded iron formations), foliated series (Tonalite –Trondhjemite-Granodiorite (TTG), gneiss), and magmatic rocks (augen metadiorites, granodiorites and synites) (Lerouge *et al*., 2006; Owona *et al*., 2013; Ndema Mbongue *et al*., 2015). The late magmatic rocks are represented by SW-NE-trending group of small intrusions extending from Lolodorf to Olama and N-S from Lolodorf to Ngog-Tos and Edea (Ebah Abeng *et al*., 2012, Ako *et al*., 2015) (Figure 3) while the surrounding formations of greenstone belt are made up of gneiss and TTG.

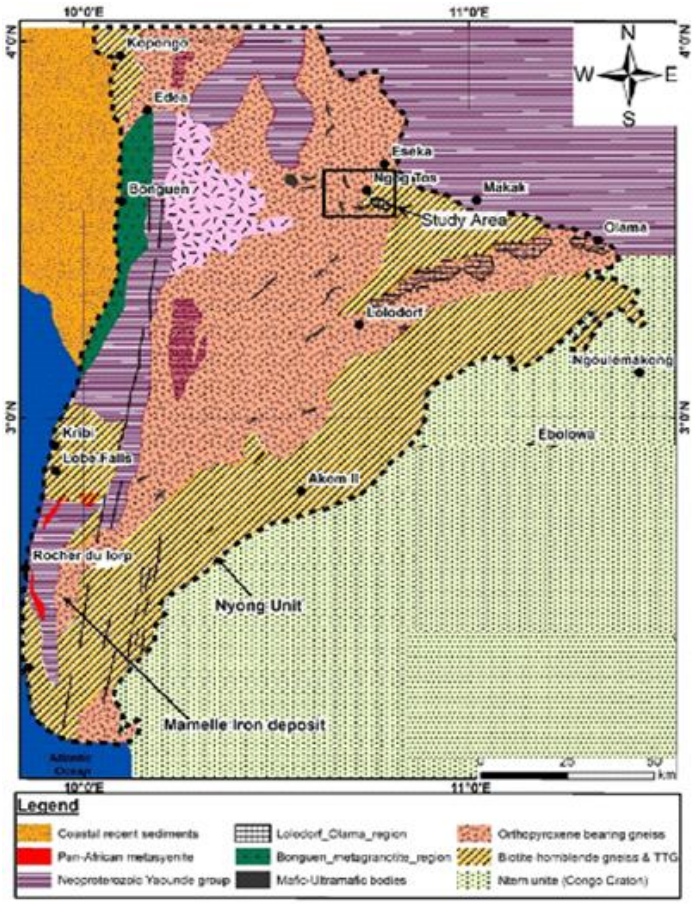


**Figure3.** *Geological map showing the late magmatic rocks that intruded the country rocks within the Nyong Series (modified after Lerouge et al., 2006; Ebah Abeng et al., 2012). Study area indicated not to scale.*

## 3. MATERIALS AND METHODS

The field study consisted of systematic mapping and sampling of lithological units of the selected area within the Nyong Series where ultramafic rocks where found. A total of twenty seven ultramafic rock samples were collected during the field work and were later used for the various analyses. Preparation of the polished thin sections was done at the University of Ghent, Belgium and studied in the laboratory of the Department of Geology, University of Buea, Cameroon. Details of these are contained in Ako *et al.*, 2015.

Twenty seven metamorphosed ultramafic rock samples were crushed using a jaw crusher with steel plates. The crushed samples were pulverized in a ball mill made up of 99.8% $Al_2O_3$ and the resulting powder was used for the various analyses. A two-step loss on ignition (LOI) was done in which powders were first heated at 105˚ C in the presence of nitrogen to drive off adsorbed water and then ignited at 1000˚C in the presence of oxygen to drive off the remaining volatile components. Details of this method are contained in Ako, 2016 and Ako *et al*., 2017a and Ako *et al*., 2017b. All the analyses were done at Acme Analytical Laboratory, Vancouver, Canada. The accuracy of the analytical results was verified through the analysis of matrix-matched reference materials, and any potential contamination during sample preparation and analysis was monitored via suitable black materials. All analytical data presented in this work passed through quality control tests to ascertain the reliability of the results.

## 4. RESULTS AND DISCUSSION

### 4.1. Field Characteristics of the Ultramafic Rocks

The study area is made up of two distinct rock units. These units are the metasedimentary unit which is represented by the talc-tremolite schists and these rocks occur as floats of blocks with fine to medium-grained texture a meta-igneous unit which is made up of amphibole-pyroxene gneiss, amphibole-garnet gneiss and biotite-garnet gneiss. These units have been intruded by ultramafic rocks which were sampled for this study. The ultramafic unit investigated is a layered sequence exposed on

a cliff face and details of the geology and petrography are contained in Ako *et al*., 2015; Ako *et al*., 2017a and Ako *et al*., 2017b and depicted in Figure 4.

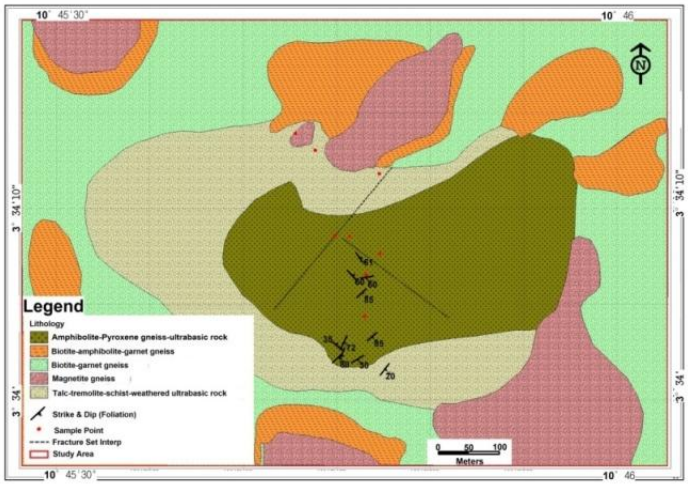


**Figure4.** *Geological map of the study area showing the various lithologies intruded by the ultramafic rocks (after Ako et al., 2015).*

## 4.2. Trace and Rare Earth Elements Geochemistry

### *4.2.1. Trace Elements*

Concentration of trace elements in the rocks greatly varies from sample to sample with some showing exceptionally high values while others show extremely very low values (Table 1). Th, U, Ta and Nb contents of the samples of the ultramafic rocks are very low and lie between 0.1 - 0.2 ppm for Th, U, and Ta, and 0.1 - 1.5 ppm for Nb while Ba concentration in many samples varies between 2 - 16 ppm except samples ESK 15 and ESK 16 which have 135 ppm and 89 ppm, respectively. The HFSE show very low to low concentrations in the samples (Sr 0.5 – 6.7 ppm, Hf 0.1 – 0.6 ppm, Zr 2 - 20.1 ppm, Y 1.4 - 44.2 ppm, Nb 0.1 - 1.5 ppm, Pb 0.6 - 11.1 ppm) (Table 1) while the large ion lithophile elements that are considered to be mobile during weathering have very low concentrations and appear to have been leached from the rocks during alteration (Bayiga *et al*., 2011). Concentration of compatible trace elements in the ultramafic rock samples like V (14 - 107 ppm) and Co (65.1 - 126.1ppm) are moderate. These compatible trace elements are considered to be relatively immobile during alteration e. g, Hébert *et al.* (1990). Therefore, they can be used as indicators of protolith composition, although it should be noted that the talc- altered ultramafic samples have low V and Co concentration, probably indicating that leaching of some of these "immobile" elements occurred during talc alteration.

**Table1.** *Trace element contents (ppm) of the ultramafic rocks in the Nyong Series*

| **Sample No.** | | **ESK 1** | **ESK 2** | **ESK 3** | **ESK 4** | **ESK 5** | **ESK 6** | **ESK 7** | **ESK 8** | **ESK 9** | **ESK 10** | **ESK 11** | **ESK 12** | **ESK 13** | **ESK 14** |
|---|---|---|---|---|---|---|---|---|---|---|---|---|---|---|---|
| **Trace elements** | **d.l** | | | | | | | | | | | | | | |
| Ba | 1 | 11 | 10 | 14 | 14 | 4 | 4 | 3 | 4 | 10 | 12 | 7 | 7 | 6 | 5 |
| Th | 0.2 | 0.8 | 0.9 | 0.9 | 1 | <0.2 | <0.2 | 0.2 | 0.3 | <0.2 | <0.2 | <0.2 | <0.2 | 0.5 | 0.7 |
| U | 0.1 | 0.2 | 0.2 | 0.2 | 0.2 | <0.1 | <0.1 | 0.1 | 0.1 | 0.2 | 0.2 | 0.2 | 0.2 | 0.2 | 0.2 |
| Nb | 0.1 | 1.5 | 1.5 | 1.1 | 1.2 | 0.5 | 0.6 | 0.8 | 0.9 | 0.3 | 0.2 | 0.4 | 0.4 | 0.7 | 0.6 |
| Pb | 0.1 | 5.2 | 5.2 | 0.8 | 0.6 | 5.6 | 5.3 | 0.8 | 0.6 | 2 | 2.2 | 4.4 | 3.9 | 2.2 | 2 |
| Sr | 0.5 | 6.7 | 6.6 | 0.9 | 0.7 | <0.5 | <0.5 | 1.3 | 1.7 | 5.8 | 5.5 | 0.9 | 0.8 | 0.8 | 0.9 |
| Zr | 0.1 | 5.7 | 5.3 | 7.7 | 7.9 | 3.5 | 3.2 | 5.8 | 5.6 | 7.7 | 8.0 | 5.5 | 5.2 | 3.2 | 3.0 |
| Sc | 1 | 9 | 8 | 11 | 11 | 9 | 9 | 8 | 9 | 8 | 9 | 9 | 8 | 10 | 9 |
| Rb | 0.1 | 1.1 | 1.3 | 1.7 | 1.9 | 0.6 | 0.7 | 0.3 | 0.2 | 0.3 | 0.4 | 0.2 | 0.5 | 0.3 | 0.2 |
| Hf | 0.1 | <0.1 | <0.1 | 0.2 | 0.2 | 0.1 | 0.1 | 0.2 | 0.2 | <0.1 | <0.1 | 0.2 | 0.1 | <0.1 | <0.1 |
| Ta | 0.1 | 0.1 | 0.1 | 0.2 | 0.1 | <0.1 | <0.1 | <0.1 | <0.1 | <0.1 | <0.1 | <0.1 | <0.1 | 0.1 | 0.1 |
| Zn | 1 | 207 | 205 | 274 | 277 | 84 | 79 | 53 | 50 | 108 | 110 | 88 | 84 | 92 | 95 |
| Mo | 0.1 | <0.1 | <0.1 | <0.1 | <0.1 | <0.1 | <0.1 | <0.1 | <0.1 | <0.1 | <0.1 | <0.1 | <0.1 | <0.1 | <0.1 |
| V | 8 | 45 | 46 | 41 | 40 | 33 | 35 | 43 | 47 | 31 | 31 | 30 | 29 | 36 | 38 |
| Co | 0.2 | 82.4 | 83.1 | 108.3 | 107.5 | 90.6 | 90.2 | 65.1 | 68.1 | 94.5 | 95 | 104 | 105.1 | 120.2 | 119.8 |

*d.l: detection limits*

**Table1.** *Trace element contents (ppm) of the ultramafic rocks in the Nyong Series (continued)*

| Sample No. | | ESK 15 | ESK 16 | ESK 17 | ESK 18 | ESK 19 | ESK 20 | ESK 21 | ESK 22 | ESK 23 | ESK 24 | ESK 25 | ESK 26 | ESK 27 |
|---|---|---|---|---|---|---|---|---|---|---|---|---|---|---|
| **Trace elements** | **d.l** | | | | | | | | | | | | | |
| Ba | 1 | 135 | 89 | 3 | 3 | 3 | 3 | 2 | 3 | 5 | 9 | 11 | 16 | 12 |
| Th | 0.2 | 0.3 | 0.3 | 0.4 | 0.3 | <0.2 | <0.2 | <0.2 | <0.2 | 0.3 | 0.4 | <0.2 | <0.2 | 0.4 |
| U | 0.1 | 0.2 | 0.2 | <0.1 | <0.1 | <0.1 | <0.1 | 0.1 | 0.1 | 0.2 | 0.2 | 0.2 | 0.2 | 0.2 |
| Nb | 0.1 | 0.3 | 0.2 | 0.8 | 0.7 | 0.1 | 0.1 | 0.2 | 0.1 | 0.3 | 0.3 | <0.1 | <0.1 | 0.7 |
| Pb | 0.1 | 5.5 | 4.9 | 4.1 | 5.2 | 0.7 | 0.7 | 10 | 11.1 | 3.7 | 3.3 | 1.2 | 1.5 | 5 |
| Sr | 0.5 | 3.6 | 3.2 | 0.6 | 0.54 | <0.5 | <0.5 | 6.4 | 6.3 | 3.1 | 3.3 | <0.5 | <0.5 | 3 |
| Zr | 0.1 | 5.4 | 5.0 | 2.0 | 2.2 | 2.3 | 2.2 | 4.4 | 4.8 | 6.9 | 6.2 | 3.8 | 3.5 | 20.1 |
| Sc | 1 | 11 | 12 | 8 | 9 | 9 | 9 | 10 | 9 | 10 | 10 | 9 | 9 | 19 |
| Rb | 0.1 | 1.2 | 1.4 | 1.5 | 1.7 | 0.6 | 0.5 | 0.2 | 0.2 | 0.4 | 0.2 | 0.3 | 0.2 | 2.9 |
| Hf | 0.1 | 0.2 | 0.1 | <0.1 | <0.1 | <0.1 | <0.1 | <0.1 | <0.1 | 0.1 | 0.1 | <0.1 | <0.1 | 0.6 |
| Ta | 0.1 | 0.1 | 0.1 | 0.1 | 0.1 | 0.1 | 0.1 | 0.1 | 0.1 | 0.1 | 0.1 | 0.1 | 0.1 | 0.1 |
| Zn | 1 | 153 | 157 | 64 | 61 | 81 | 85 | 36 | 36 | 89 | 91 | 85 | 82 | 174 |
| Mo | 0.1 | 0.2 | 0.4 | <0.1 | <0.1 | <0.1 | <0.1 | <0.1 | <0.1 | <0.1 | <0.1 | <0.1 | <0.1 | 0.1 |
| V | 8 | 45 | 42 | 26 | 23 | 16 | 14 | 30 | 32 | 54 | 59 | 37 | 33 | 107 |
| Co | 0.2 | 96 | 96.1 | 92.3 | 92.2 | 82.5 | 81.9 | 116.9 | 121 | 119.7 | 124 | 93 | 98 | 126.1 |

*d.l: detection limits*

All the samples from the study area define a light trend on a (Nb/Th) vs (Th/Yb) plot, and have low ( Nb/Th) average ratio of 0.6 and elevated (Th/Yb) average ratio of 1.0 .These two characteristics, i.e. ( Nb/Th) < 1 and (Th/Yb) >1, are generally accepted to be the product of crustal contamination of mantle-derived magmas (Ihlenfeld and Keays, 2011; Lightfoot *et al.*, 1990; Lightfoot and Hawkesworth, 1997). This illustration is in agreement with the results recorded in the pyroxenites and amphibolites of Lolodorf, Kabaga nickel sulphide deposits, Kalotongke Ni-Cu deposits and the Nuashai massif gabbro-breccia zone (Figure 5a). The composition characteristics of the samples are highlighted in the ratio diagrams of incompatible elements (Figure 5b, c and d).

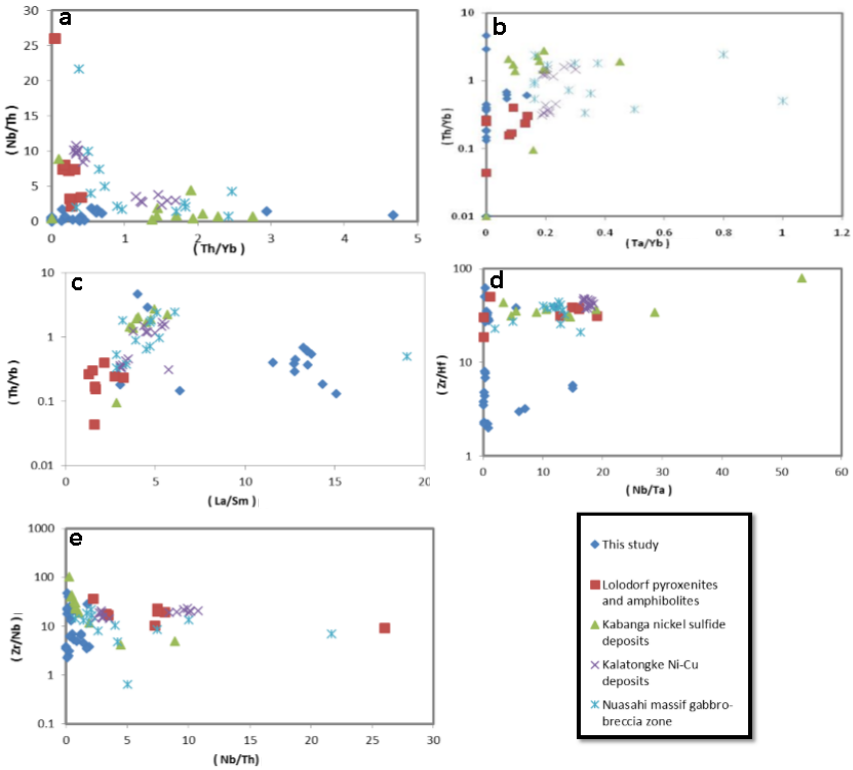


**Figure5.** *Scatter plots of trace element ratios showing the compositional characteristics of the ultramafic rocks of the Nyong Series with comparable studies in other parts of the world*

On the (Th/Yb) vs ( Ta/Yb ) plot, the ultramafic rock samples show moderate to high Th/Yb ratios and very low Ta/Yb ratios which are similar to comparable samples except a few samples from the Nuasahi Massif gabbro-breccia and Kabanga nickel sulphide deposits that show both moderate to high

Th/Yb and Ta/Yb ratios(Figure 5b). In a like manner, on the Th/Yb vs La/Sm plot, the studied samples show moderate to high Th/Yb ratios and low to high La/Sm ratios. These ratios are similar to other comparable studies (Figure 5c).

Fifteen of the samples have very low Zr/Hf ratios of between 2-8 (except samples ESK 3, 4, 5, 6, 7, 8, 11, 12, 15, 16, 24 and 27 which have 38.5, 39.5, 35, 32, 29, 28, 27.5, 52, 27, 50, 62 and 35.5 respectively) and very low Nb/Ta ratios between 0.1-15. Other comparable rocks however show very high Zr/Hf ratios but low-moderate Nb/Ta ratios (Figure 5d). On the (Zr/Nb) vs Nb/Th plot, the samples show very low Nb/Th ratios and moderate Zr/Nb ratios while comparable samples show moderate Nb/Th ratios and moderate to high Zr/Nb ratios (Figure 5e).

In the Zr vs Nb and La bivariate plots, there is a corresponding increase in the Nb values with a very narrow range in the Zr values. The zig-zag patterns of the scatter graph for the ultramafic rock samples reflect slightly both positive and negative correlations but other related rocks from other parts of the world show positive correlations (Figure 6a and b) while in the Sr vs Zr plot, the Sr/Zr values are very low without any correlation but other comparable samples show high values with positive correlations (Figure 6c). Zr is a very incompatible element that does not substitute in major silicate phase (although they may replace Ti in titanite or rutile) and its low concentrations in the samples imply a depleted source or limited liquid evolution while Sr substitutes for Ca in plagioclase (but not in pyroxene) and to a lesser extent, for K in K-feldspar and as a compatible element at low pressure where plagioclase forms early, but as an incompatible element at higher pressure where plagioclase is no longer stable (Winter, 2001).

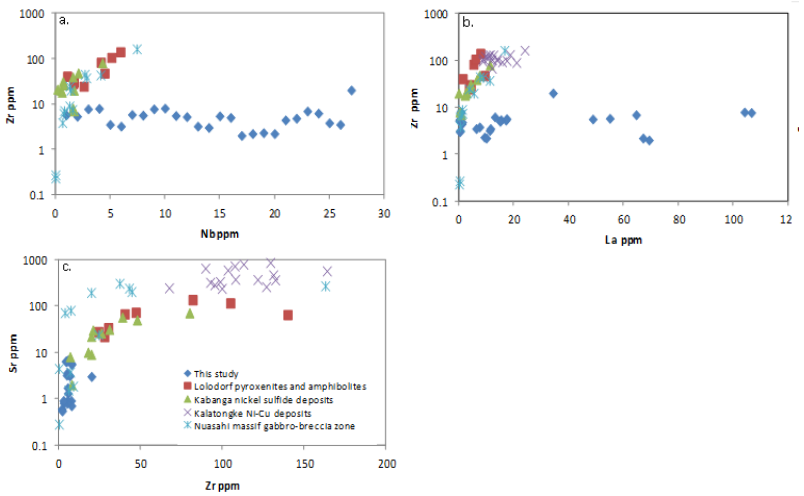


**Figure6.** *Bivariate plots (a) Zr/Nb, (b) Zr/La and (c) Sr/Zr of the ultramafic rocks of the Nyong Series with comparable studies in other parts of the world*

Both Zr and Sr are high-field strength elements (HFSEs) and are supposed to be immobile during low grade metamorphism, weathering and hydrothermal alterations (Pearce and Cann, 1973; Winchester and Floyd, 1976a and b; Floyd and Winchester, 1978; Rollinson, 1993; Jochum and Verma, 1996).

The representative primitive mantle normalized trace elements spider plots (after Jochum *et al.*, 1988 and McDonough and Sun, 1995) for the ultramafic rock samples are presented in Figure 7. Relative to the primitive mantle, the rocks show relative enrichment of LILEs (such as Sc, Rb, Ba, Th and U) with very steep slopes and depletion of HFSE (such as Ta and Nb) which also show very steep and gentle slopes respectively. They are further characterized by distinct troughs such as Ta-Nb and Sr-Nb. These features are characteristics of tholeiitic basalts produced at destructive plate margins or within plate tholeiites contaminated by continental crust (Hawkesworth *et al.*, 1994; Taylor and McLennan, 1985) whereas the flat patterns of the other incompatible trace elements are normally interpreted to reflect magma generation in the depleted mantle (Figure 7). Almost all the samples have highly anomalous spidergram patterns with distinct and variable Ba, Th, Hf and Zr anomalies and indicate depletion of HFSEs (Ta, Sr, Hf, Zr, Nb) and positive anomalies for Rb, Th, U, Nb and Pb. Mondal and Zhou (2010) have reported negative Nb, Th, Zr and Hf anomalies in gabbro and breccias in the Nuasahi Massif indicating derivation from a depleted mantle source. Samples of the ultramafic units have a narrow range of incompatible trace element ratios indicating a cogenetic relationship. The

ultramafic rocks and the gabbros relatively constant subcondritic Nb/Ta ratios (ultramafic rocks: Nb/Ta = 4.1 - 8.8; gabbro unit: Nb/Ta = 11.5-13.2), whereas samples of the breccias zone are characterized by highly variable Nb/Ta ratios (Nb/Ta = 2.5-16.6) and show evidence of metasomatism. The enrichment of light rare earth elements and mobile incompatible elements in the mineralized samples provides supporting evidence for metasomatism.

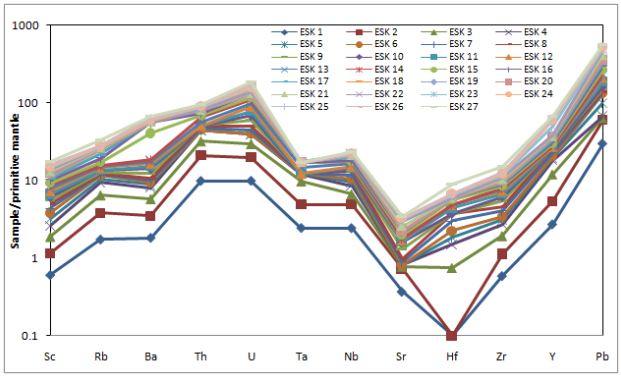


**Figure7.** *Primitive-mantle normalized trace element patterns for the representative rock samples from the Nyong Series.*

### *4.2.2. Rare Earth Elements (REEs)*

The REEs data for the ultramafic rock samples are presented in Table 2. REEs concentrations are more or less radon in the samples and they vary from 0.05 – 106.7 ppm. La and Nd show relatively higher concentrations compared to the other REEs. Tb, Eu (except ESK 3, 4, 18, 27), Tm and Lu all have concentrations of less than 1ppm while La (0.6 – 93.2 ppm), Ce (0.6 – 93.2 ppm), Sm (0.07 - 7.94 ppm), Gd(0.19 - 6.01ppm), Dy (0.13 - 5.01ppm), Ho (0.03 - 1.12 ppm) Er (0.01 - 3.39ppm), Tb, (0.14 - 2.73) all have average concentrations that are >1ppm (Table 2). Total REE (ΣREE) concentrations in the samples range from 2.55 – 252.2 ppm with an average of 74.05 ppm while LREEs and HREEs concentrations range from 1.65 – 236.95 ppm and 0.85 – 18.34 ppm with averages of 69.65 ppm and 6.39ppm respectively. The samples are enriched in LREEs (LREE/HREE >1). Average Eu* and Ce* values in the samples are 0.72 and 1.87 respectively while average $La/Yb_N$ is 0.79 (Table 2).

Primitive mantle normalised REE plots (after Jochum *et al*., 1989 and Hofmann, 1989) of the ultramafic rocks are characterized by four distinct types of patterns based on their shapes and Eu anomalies (Eu*) (Figure 8a - d). Tpye 1 samples are characterized by steep LREE patterns, slightly positive Eu* and flat HREE patterns (Figure 8a). Type 2 exhibit LREE patterns with high peak values for La and Pr, V-shape Ce anomaly, a very gentle HREE pattern and a moderate negative Eu*(Figure 8b). Type 3 samples show a steep LREE patterns, strong negative Eu* and flat HREE patterns (Figure 8c) whereas Type 4 samples display flat and very steep LREE patterns, a very strong negative Eu* and a very flat HREE patterns (Figure 8d). Generally all the four types are characterized by enrichment in LREEs and depletion in HREEs and a negative Eu and Ce anomalies except the type 1. Primitive mantle normalised REE plots of samples from other studies in other parts of the world show similar enrichment in LREEs but flat HREE patterns except the Kabanga and Platreef sulfide deposits which show enrichments in Lu and Ho, respectively (Figure 9).

**Table2.** *Rare earth elements (REE) contents (ppm) of the ultramafic rocks in the Nyong Series*

| Sample No. | | ESK 1 | ESK 2 | ESK 3 | ESK 4 | ESK 5 | ESK 6 | ESK 7 | ESK 8 | ESK 9 | ESK 10 | ESK 11 | ESK 12 | ESK 13 | ESK 14 | ESK 15 |
|---|---|---|---|---|---|---|---|---|---|---|---|---|---|---|---|---|
| **REE** | **d.l** | | | | | | | | | | | | | | | |
| La | 0.1 | 17.5 | 17.2 | 106.7 | 104.2 | 11.6 | 11.3 | 55.1 | 48.9 | 0.8 | 0.7 | 0.3 | 0.2 | 0.5 | 0.4 | 15.4 |
| Ce | 0.1 | 15.4 | 15.2 | 38.2 | 37.8 | 11.4 | 10.9 | 3.3 | 3.2 | 0.9 | 0.8 | 0.6 | 0.6 | 0.9 | 1.1 | 43.1 |
| Pr | 0.02 | 2.52 | 2.5 | 21.21 | 21.11 | 1.84 | 1.82 | 9.65 | 9.8 | 0.19 | 0.2 | 0.08 | 0.08 | 0.12 | 0.11 | 2.54 |
| Nd | 0.3 | 7.6 | 7.5 | 61.5 | 59.9 | 5.7 | 5.7 | 31.8 | 32.1 | 1.1 | 1.1 | 0.6 | 0.9 | 0.9 | 0.9 | 8.2 |
| Sm | 0.05 | 1.28 | 1.28 | 7.94 | 7.88 | 0.78 | 0.77 | 3.85 | 3.83 | 0.1 | 0.13 | 0.07 | 0.07 | 0.11 | 0.1 | 1.21 |
| Eu | 0.02 | 0.22 | 0.22 | 1.4 | 1.38 | 0.14 | 0.17 | 0.72 | 0.72 | <0.02 | <0.02 | <0.02 | <0.02 | <0.02 | <0.02 | 0.54 |
| Gd | 0.05 | 1.57 | 1.5 | 6.01 | 5.99 | 0.76 | 0.72 | 3.21 | 3.31 | 0.31 | 0.29 | 0.19 | 0.21 | 0.27 | 0.25 | 1.3 |
| Tb | 0.01 | 0.29 | 0.28 | 0.89 | 0.88 | 0.13 | 0.17 | 0.49 | 0.36 | 0.04 | 0.03 | 0.03 | 0.03 | 0.04 | 0.03 | 0.22 |

| | | | | | | | | | | | | | | | | |
|---|---|---|---|---|---|---|---|---|---|---|---|---|---|---|---|---|
| Dy | 0.05 | 1.75 | 1.72 | 3.91 | 3.89 | 0.5 | 0.41 | 2.51 | 2.5 | 0.45 | 0.51 | 0.18 | 0.13 | 0.41 | 0.38 | 1.24 |
| Ho | 0.02 | 0.34 | 0.33 | 0.89 | 0.85 | 0.16 | 0.18 | 0.51 | 0.57 | 0.06 | 0.03 | 0.05 | 0.04 | 0.08 | 0.08 | 0.31 |
| Er | 0.03 | 1.21 | 1.19 | 2.17 | 2.19 | 0.33 | 0.35 | 1.32 | 1.35 | 0.26 | 0.23 | 0.15 | 0.11 | 0.27 | 0.3 | 0.82 |
| Tm | 0.01 | 0.21 | 0.24 | 0.28 | 0.24 | 0.06 | 0.03 | 0.17 | 0.11 | 0.04 | 0.07 | 0.02 | 0.02 | 0.03 | 0.01 | 0.11 |
| Yb | 0.05 | 1.46 | 1.44 | 1.47 | 1.46 | 0.36 | 0.39 | 1.06 | 1.04 | 0.14 | 0.16 | 0.24 | 0.27 | 0.17 | 0.15 | 0.78 |
| Lu | 0.5 | 0.19 | 0.19 | 0.24 | 0.27 | 0.05 | 0.08 | 0.15 | 0.12 | 0.04 | 0.06 | 0.04 | 0.04 | 0.03 | 0.04 | 0.11 |
| ∑REE | - | 51.54 | 50.79 | 252.81 | 248.04 | 33.81 | 32.99 | 113.84 | 107.91 | 4.43 | 4.31 | 2.55 | 2.7 | 3.83 | 3.85 | 75.88 |
| LREE | - | 44.52 | 43.9 | 236.95 | 232.27 | 31.46 | 30.66 | 104.42 | 98.55 | 3.09 | 2.93 | 1.65 | 1.85 | 2.53 | 2.61 | 70.99 |
| HREE | - | 7.02 | 6.89 | 15.86 | 15.77 | 2.35 | 2.33 | 9.42 | 9.36 | 1.34 | 1.38 | 0.9 | 0.85 | 1.3 | 1.24 | 4.89 |
| Ce/Ce* | - | 1.57 | 1.58 | 0.8 | 0.55 | 1.68 | 1.63 | 0.1 | 0.1 | 1.53 | 1.47 | 2.7 | 3.18 | 2.48 | 3.56 | 4.7 |
| Eu/Eu* | - | 0.54 | 0.55 | 0.7 | 0.7 | 0.63 | 0.89 | 0.37 | 0.7 | - | - | - | - | - | - | 1.5 |
| $(La/Yb)_N$ | - | 0.4 | 0.4 | 0.59 | 2.4 | 1.08 | 1.05 | 1.75 | 2.14 | 0.19 | 0.15 | 0.4 | 0.03 | 0.1 | 0.09 | 0.66 |

*d.l: detection limits*

$Ce/Ce^* = (Ce_{sample}/Ce_{primitive\ mantle})/(La_{sample}/La_{primitive\ mantle})^{1/2}\ (Pr_{sample}/Pr_{primitive\ mantle})^{1/2}$

$Eu/Eu^* = (Eu_{sample}/Eu_{primitive\ mantle})\ /(Sm_{sample}/Sm_{primitive\ mantle})^{1/2}\ (Gd_{sample}/Gd_{primitive\ mantle})^{1/2}$

$(La/Yb)N = (La_{sample}/La_{primitive\ mantle})/Yb_{sample}/Yb_{primitive\ mantle})$

**Table2.** *Rare earth elements (REE) contents (ppm) of the ultramafic rocks in the Nyong Series (continued)*

| **Sample No.** | | **ESK 16** | **ESK 17** | **ESK 18** | **ESK 19** | **ESK 20** | **ESK 21** | **ESK 22** | **ESK 23** | **ESK 24** | **ESK 25** | **ESK 26** | **ESK 27** |
|---|---|---|---|---|---|---|---|---|---|---|---|---|---|
| **REE** | **d.l** | | | | | | | | | | | | |
| La | 0.1 | 15.1 | 69.4 | 67.2 | 9.4 | 10.1 | 1.1 | 1.3 | 64.7 | 13.2 | 7.6 | 6.4 | 34.4 |
| Ce | 0.1 | 41.9 | 36 | 35.8 | 6.6 | 5.5 | 1.7 | 1.5 | 5 | 4.8 | 24.8 | 24.9 | 93.2 |
| Pr | 0.02 | 2.51 | 16.04 | 16 | 1.41 | 1.44 | 0.23 | 0.21 | 9.39 | 9.36 | 1.68 | 1.7 | 10.51 |
| Nd | 0.3 | 8.4 | 51.1 | 50.8 | 4.1 | 3.9 | 1.1 | 1.3 | 34 | 33.8 | 5.1 | 5.3 | 31.7 |
| Sm | 0.05 | 1.31 | 5.42 | 4.99 | 0.7 | 0.71 | 0.37 | 0.37 | 4.29 | 4.33 | 0.92 | 1 | 5.4 |
| Eu | 0.02 | 0.49 | 0.94 | 1.1 | 0.11 | 0.11 | <0.02 | <0.02 | 0.82 | 0.85 | 0.18 | 0.12 | 1.03 |
| Gd | 0.05 | 1.33 | 3.49 | 3.37 | 0.62 | 0.59 | 0.52 | 0.45 | 4.98 | 4.88 | 0.88 | 0.82 | 4.07 |
| Tb | 0.01 | 0.027 | 0.44 | 0.47 | 0.13 | 0.1 | 0.08 | 0.05 | 0.81 | 0.78 | 0.18 | 0.14 | 0.77 |
| Dy | 0.05 | 1.2 | 2 | 1.99 | 0.83 | 0.79 | 0.51 | 0.49 | 4.98 | 5.01 | 1.15 | 0.91 | 4.79 |
| Ho | 0.02 | 0.28 | 0.37 | 0.39 | 0.18 | 0.13 | 0.11 | 0.19 | 1.12 | 0.91 | 0.28 | 0.22 | 0.9 |
| Er | 0.03 | 0.87 | 0.73 | 0.69 | 0.37 | 0.34 | 0.38 | 0.4 | 3.39 | 3.35 | 0.77 | 0.8 | 2.47 |
| Tm | 0.01 | 0.15 | 0.12 | 0.09 | 0.08 | 0.1 | 0.05 | 0.06 | 0.4 | 0.39 | 0.1 | 0.9 | 0.39 |
| Yb | 0.05 | 0.74 | 0.89 | 0.82 | 0.45 | 0.48 | 0.35 | 0.33 | 2.28 | 2.2 | 0.75 | 0.72 | 2.73 |
| Lu | 0.5 | 0.17 | 0.13 | 0.11 | 0.06 | 0.09 | 0.05 | 0.05 | 0.38 | 0.29 | 0.09 | 0.07 | 0.43 |
| ∑REE | - | 74.477 | 187.07 | 183.82 | 25.04 | 24.38 | 6.55 | 6.7 | 136.54 | 84.15 | 44.48 | 44 | 192.79 |
| LREE | - | 69.71 | 178.9 | 175.89 | 22.32 | 21.76 | 4.5 | 4.68 | 118.2 | 66.34 | 40.28 | 39.42 | 176.24 |
| HREE | - | 4.676 | 8.17 | 7.93 | 2.72 | 2.62 | 2.05 | 2.02 | 18.34 | 17.81 | 4.2 | 4.58 | 16.55 |
| Ce/Ce* | - | 0.001 | 2.2 | 0.74 | 1.24 | 0.98 | 2.3 | 1.87 | 0.104 | 0.3 | 4.71 | 5.1 | 3.33 |
| Eu/Eu* | - | 1.67 | 0.48 | 0.93 | 0.0005 | 0.59 | | | 0.62 | 0.64 | 0.95 | 0.5 | 0.76 |
| (La/Yb)N | - | 1.05 | 2.62 | 2.75 | 0.7 | 0.7 | 0.11 | 0.13 | 0.95 | 0.2 | 0.02 | 0.3 | 0.42 |

*d.l: detection limits*

$Ce/Ce^* = (Ce_{sample}/Ce_{primitive\ mantle})/(La_{sample}/La_{primitive\ mantle})^{1/2}\ (Pr_{sample}/Pr_{primitive\ mantle})^{1/2}$

$Eu/Eu^* = (Eu_{sample}/Eu_{primitive\ mantle})\ /(Sm_{sample}/Sm_{primitive\ mantle})^{1/2}\ (Gd_{sample}/Gd_{primitive\ mantle})^{1/2}$

$(La/Yb)_N = (La_{sample}/La_{primitive\ mantle})/Yb_{sample}/Yb_{primitive\ mantle})$

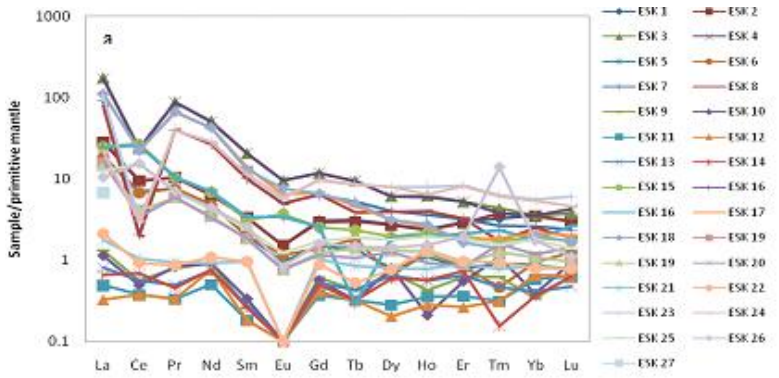

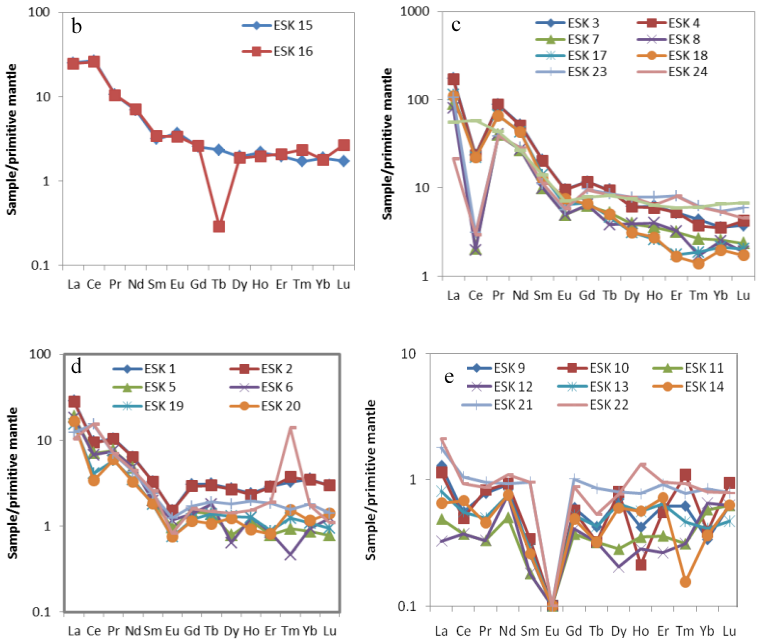


**Figure8.** *(a) Primitive mantle normalized REE plots of the ultramafic rocks of the Nyong Series showing four distinct types of patterns based on their shapes and Eu anomalies (Eu*). (b) Type 1 is characterized by steep LREE patterns, slightly positive Eu* and flat HREE patterns. (c) Type 2 exhibits LREE patterns with high peak values for La and Pr, V-shape Ce anomaly, a very gentle HREE pattern and a moderate negative Eu*. (d) Type 3 samples show a steep LREE patterns, strong negative Eu* and flat HREE patterns. (e) Type 4 samples display flat and very steep LREE patterns, a very strong negative Eu* and a very flat HREE patterns*

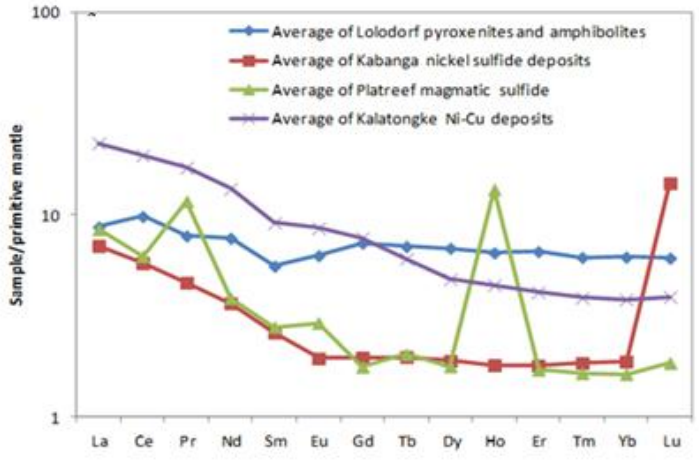


**Figure9.** *Primitive mantle normalized REE plots of samples from other studies in other parts of the world show similar enrichment in LREE but flat HREE patterns except the Kabanga and Platreef sulfide deposits which show enrichments in Lu and Ho respectively*

These trends in the REE patterns can be interpreted that these trends are the result of fractional crystallization and fractionation of the LREEs relative to the heavy ones may be caused by the presence of olivine, orthopyroxene and clinopyroxene. Generally, the nature of these patterns suggests complete evolution of the Nyong ultramafic rocks through multiple magmatic processes associated with crustal contamination in the magma in subsequent stages (Balaram *et al*., 2013).

The nature of the patterns suggests complex evolution of these ultramafic rocks through multiple magmatic processes associated with crustal contamination in the magma in subsequent stages. The negative Eu anomalies in the samples may be interpreted as due to fractionation of plagioclase ± hornblende and can be imposed when the melt phase enters the stability field of plagioclase. Low CaO, $Al_2O_3$ and Sr (Ding *et al*., 2012; Dare *et al*., 2014; Barnes *et al*., 2015; Ako, 2016 and Ako *et al*., 2017a) contents and negative Eu anomaly are all features that suggest removal of plagioclase component from the basic magma or may be due to the magma that might have segregated at such

depth where plagioclase is not stable and hence it could not be fractionated (Barker *et al.,* 1976). Eu anomalies are chiefly controlled by feldspars; particularly in felsic magma for Eu (present in the divalent state) is compatible in plagioclase and K-feldspar, in contrast to the trivalent REE which are incompatible. Thus a removal of feldspar from a melt by crystal fractionation or the partial melting of a rock in which feldspar is retained in the source will give rise to a negative Eu* in the melt. To a lesser extend hornblende, sphene, clinopyroxene, orthopyroxene and garnet may also contribute to Eu*, although in the opposite sense to that of feldspars (Hugh, 1993).

The high LREE contents in the rocks could be related to the enrichment of their source materials or to low degree of partial melting of source protoliths (Figure 8a) with which garnet was among the residual phases (Nzenti *et al.,* 2006). The negative Ce and Eu anomalies probably result from the variability of oxidizing conditions (Neal and Taylor, 1989). The negative Ce anomalies in some samples are similar to those of the Kabanga Ni sulphide deposits in Tanzania (Maier *et al.,* 2010). The negative Eu anomalies could result from the high degree of plagioclase fractionation (Lee *et al.,* 2009; Saleh, 2007). According to Lee *et al.* (2009) large amount of plagioclase growth removes significant $Eu^{2+}$ from the system during magma crystallization and this reduction of total Eu limits available zircon, resulting in progressively more negative anomalies in later grown zircon. The variability of $(La/Yb)_N$ ratios in the rocks could be relative to the early stage weathering.

## 5. CONCLUSION

The metamorphosed ultramafic rocks of the Paleoproterozoic Nyong Series SE Cameroon are characterised by relative enrichment in LILE (e.g. Ba, Th and U) and depleted in HFSE (e.g. Sr, Zr, Nb and Hf). They also show negative Ce and Eu anomalies. Four distinct types of primitive mantle normalized REE patterns based on the shapes and degree of Eu anomaly are recognized. Generally, the four patterns are characterized by enrichment in LREEs and depletion in HREEs. The low Sr, Zr, Nb and Hf contents and negative Eu anomaly are all features that suggest removal of plagioclase component from the basic magma or may be due to the magma that might segregated at depth where plagioclase is not stable and thus could not have fractionated.

Rare earth elements are reliable petrogenetic indicators and have unique properties such as strong electropositive character, constancy in valance state (3+) with exception of Eu and Yb showing additional (2+) and Ce and Tb showing additional (4+) valence. They display significant substitution especially of tetravalent cations in different minerals and systematic partitioning in the mineral/melt systems. REEs (especially LREEs) are among the most incompatible elements and therefore enrich the magmas having low degrees of partial melting and metasomatised source rocks. Behavior of REEs in metamorphic rocks depends on their protolith and P-T-X conditions and accessory minerals such as garnet, zircon, monazite, sphene, apatite and quartz, greatly influence REEs distribution within metamorphic rocks.

## ACKNOWLEDGEMENT

This article is part of the PhD thesis of the first author supervised by Prof. C. E. Suh (CES) at the University of Buea, Cameroon and completed within the research framework of economic geology on the Precambrian Mineral belt of Cameroon supported by University of Buea, Faculty Grants to CES. We gratefully acknowledge funding from the AvH Stiftung, Germany (courtesy of CES) and the Research grant in support of this thesis from the national body of Academic Staff Union of Universities (ASUU, Nigeria).

## REFERENCES

[1] Ako, T. A. (2016). Petrochemistry of Metamorphosed Ultramafic Rocks in the Paleoproterozoic Nyong Series (SE Cameroon) and their bearing on Platinum Group Elements (PGEs) Mineralisation. PhD Thesis, University of Buea, Cameroon, 180pp.

[2] Ako, T. A., Vishiti, A., Ateh, K. I., Kedia, A. C. and Suh, C. E. (2015). Mineral Alteration andChlorite Geothermometry in Platinum Group Element (PGE)-bearing meta-ultramafic rocks from South East Cameroon. Journal of Geosciences and Geomatics, 3 (4): 96-108.

[3] Ako, T. A., Vishiti, A., Suh, C. E. and Kedia, A. C. (2017a). Evaluation of Platinum Group Elements (PGE) Potentials of Ultramafic rocks of the Paleoproterozoic Nyong Series, Southeast Cameroon. International Journal of Mining Science (IJMS), Vol. 3, Issue 3, Pp 21-39.

[4] Ako, T. A., Vishiti, A., Suh, C. E. and Kedia, A. C. (2017b). Geological Models of Platinum Group Elements (PGE) Depletion in Metamorphosed Ultramafic Rocks of the Nyong Series, Southeast Cameroon. International Journal of Mining Science (IJMS), Vol. 3, Issue 4, Pp 52 – 63.

[5] Ako, T. A., Vishiti, A.,Ateh, K. I., Kedia, A. C. and Suh, C. E. (2015). Mineral Alteration and Chlorite Geothermometry in Platinum Group Element (PGE)-bearing meta-ultramafic rocks from South East Cameroon. Journal of Geosciences and Geomatics, 3(4): 96-108.

[6] Balaram, V., Singh, S. P., Satyanarayanan, M. and Anjaiah, K. V. (2013). Platinum group elements geochemistry of ultramafic and associated rocks from Pindar in Madarawa Igneous Complex, Bundlkhand massif, Central India. Journal of Earth System Sciences, 122 (1): 79-91.

[7] Barnes, S-J., Pagé, P., Prichand, H. M., Zientek, M. I. and Fisher, P. C. (2015). Chalcophile and platinum-group element distribution in the Ultramafic series of the Stillwater Complex, MT, USA – Implications for processes enriching chromite layers in Os, Ir, Ru and Rh. Mineralium Deposita, (doi:10.1007/s00126-015-0587-y) Retrived online on 10/08/15.

[8] Bayiga, E. C., Bitom, D., Ndjigui, P.-D. and Bilong, P. (2011). Mineralogical and geochemical characterization of weathering products of amphibolites at SW Eséka (Northern border of the Nyong unit, SW Cameroon). Journal of Geology and Mining Research, 3 (10): 281-293.

[9] Bonhomme, M. G., Gauthier-Lafaye, F. and Weber, F. (1982). An example of Lower Proteroizoic sediments: the Francevillian in Garbon. Precambrian Research, 18: 87–102.

[10] Boynton, W.V. (1989). Cosmochemistry of the rare earth elements: condensation and evaporation processes. In: B.R. Lipin and G.A. McKay (Eds.), Geochemistry and Mineralogy of Rare Earth Elements. Rev. Mineral., v.21, pp.1-24.

[11] Dare, S. A. A., Barnes, S-J., Prichard, H., and Fisher, P. C. (2014). Mineralogy and geochemistry of Cu-rich ores from the McCreedy East Ni-Cu-PGE Deposit (Sudbury, Canada): Implications for the behavior of platinum group and chalcophile elements at the end of crystallization of a sulfide liquid. Economic Geology,109 (2): 343-366.

[12] Ding, X., Ripley, E. M. and Li, C. (2012). PGE geochemistry of the Eagle Ni-Cu-(PGE) deposit, Upper Michigan: constraints on ore genesis in a dynamic magma conduit. Mineralium Deposita, 47: 89-104.

[13] Ebah Abeng, A. S., Ndjigui, P-D., Beyanu, A. A., Tessontsap, T. and Bilong, P. (2012). Geochemistry of pyroxenites, amphibolites and their weathered products in the Nyong unit, SW Cameroon (NW border of Congo Craton): Implications for Au-PGE exploration. Journal of Geochemical Exploration, 114: 1 – 19.

[14] Ferry, J. M. (1982). CharacteriSation of metamorphism through mineral equilibria. Rev. Mineral., v.10, 397p

[15] Feybesse, J. L., Barbosa, J., Ledru, P., Guerrot, C., Jahan, V, Trboulet, V., Bouchot, V., Prian, J. P. and Sabaté, P. (1998). Paleoproterozoic tectonic regime and makers of the Archaean/proterozoic boundary in the Congo-São Francisco craton. EUG 8, Terra abstracts, 100.

[16] Feybesse, J. L., Johan, V., Maurizot, P. and Abessol, A. (1986). Evolution tectono-métamorphique libérenne et éburnéenne á la partie NW du craton zaïrọis (SW Cameroon). Current Research In Africa Journal of Earth Sciences, Matheis and Schandelmeier (eds) Balkema, Rotterdam: 9 – 12.

[17] Fleischer, M. and Aultschuler, Z.S. (1969). The relationship of the rare-earth composition of minerals to geologic environment. Geochim. Cosmochim. Acta, v.33, pp.725-732.

[18] Floyd, P. A. and Winchester, J. A. (1978). Identification and discrimination of altered and metamorphosed volcanic rocks using immobile elements. Chemical Geology, 21: 291-306.

[19] Hébert, R., Adamson, A. C. and Komor, S. C. (1990). Metamorphic petrology of ODP Leg 109, Hole 670A serpentinized peridotites: serpentinization processes at a slow spreading ridge environment. In Detrick, R., Honnorez, J., Bryan, W.B., Juteau, T., et al., Proc. ODP, Science Results, 106/109: College Station, TX (Ocean Drilling Program), 103–115.

[20] Henderson, P. (1984). Rare Earth Element Geochemistry. Elsevier, Amsterdam, 510p.

[21] Hofmann, A. W. (1989). Chemical differentiation of the Earth: the relationship between mantle, continental crust, and oceanic crust: Earth and Planetary Science Letters, 90: 297-314.

[22] Hugh R. R. (1993). Using geochemical data: Evaluation, Presentation and Interpretation. Pearson Education Limited, Edinburgh Gate, 380pp.

[23] Ihlenfeld, C. and Keays, R. R. (2011). Crustal contamination and PGE mineralization in the Platreef, Bushveld Complex, South Africa: evidence for multiple contamination events and transport of magmatic sulfides. Mineraliun Deposita, 46:813-832

[24] Jensen, B.B. (1973). Patterns of trace element partitioning. Geochim. Cosmochim. Acta, v.37, pp.2227-2242

[25] Jochum, K. P. and Verma, S. P. (1996). Extremely high enrichment of Sb, Ti and other trace elements in altered MORB. Chemical Geology, 130: 289–299.

[26] Jochum, K. P., McDonough, W. F., Palme, H. and Spettel, B. (1989). Compositional constraints on the continental lithospheric mantle from trace elements in spinel peridotite xenoliths. Nature, 304: 548-550.

[27] Jochum, K. P., Seufert, H. M., Midnet-Best, S., Rettmann, E., Schönberger, K. and Zimmer, M. (1988). Multi-element analysis by isotope dilution-spark source mass spectrometry (IDSSMS). Fresenius Annals of Chemistry, 331: 104-110.

[28] Lasserre, M. and Soba, D. (1976). Age libérien de granodiorites et des gneiss à pyroxene du Cameroon méridional. Bullutin, B.R.G.M. 2è série, section IV (I): 17 – 32.

[29] Lee, R. G., Dilles, J. H., Mazdab, F. K. and Wooden, J. L. (2009). Europium anomalies in Zircon from granodiorite porphyry intrusios at the El Salvador porphyry copper deposit, Chile. The Geological Society of America, 158 (8).

[30] Lerouge, C., Cocherie, A., Toteu, S. F., Penaye, J., Mile'si. J., Tchameni. R., Nsifa, E. N. Fanning, C. M. and Deloule, E. (2006). Shrimp U-Pb Zircon age for Paleoproterozoic sedimentation and 2.05Ga syntectonic plutonism in the Nyong Group, South-Western Cameroon: consequences for the Eburnean – Transamazonian belt of NE Brazil and Central Africa. Journal of African Earth Sciences, 44(4/5): 413-427.

[31] Lightfoot, P. C. and Hawkesworth, C. J. (1997). Flood basalts and magmatic Ni, Cu, and PGE sulphide mineralization: comparative geochemistry of the Noril'sk (Siberian Traps) and West Greenland sequences, in Mahoney, J. J., and Coffin, M. F., eds., Large igneous provinces: continental, oceanic and planetary flood volcanism: American Geophysical Union, Monograph 100: 357-380.

[32] Lightfoot, P. C., Naldrett, A. J., Gorbachev, N. S. and Fedorenko, V. A. (1990). Geochemistry of the Siberian trap of the Noril'sk area, USSR, with implications for the relative contributions of crust and mantle to flood basalt magmatism: Contributions to Mineralogy and Petrology, 104: 631-644.

[33] Maier, W. D., Barnes, S-J., Sarkar, A., Ripley, E., Li, C. and Livesey, T. (2010). The Kabanga Ni Sulfide deposit, Tanzania: 1. Geology, petrography, silicate rock geochemistry, and sulfur and oxygen isotopes. Mineralium Deposita, 45: 419 - 441.

[34] Maurizot, P., Abessolo, A., Feybesse, A., Johan, V. and Lecomte, P. (1986). Etude et prospection minière du sud-Ouest Cameroon. Sythèse des travaux de 1978 á 1995. 85-CMR 066 BRGM.

[35] McDonough, W. W. and Sun, S. S. (1995). The composition of the Earth. Chemical Geology, 120: 223-253.

[36] Miyashiro, A. (1973). Metamorphism and metamorphic belts. John Wiley & Sons, New York, 492p.

[37] Mondal, S. K. and Zhou, M. F. (2010). Enrichment of PGE through interaction of evolved boninitic magmas with early formed cumulates in a gabbro-breccia zone in the Mesarchaean Nuasahi massif (eastern India). Mineralium Deposita, 45(1), 69-91.

[38] Ndema Mbongue, J. L., Ngnotue, T., Ngo Nlend, C. D., Nzenti, J. P. and Cheo Suh, E. (2014). Origin and Evolution of the Formation of the Cameroon Nyong Series in the Western Border of the Congo Craton. Journal of Geosciences and Geomatics, 2(2): 62- 75.

[39] Neal, C. R. and Taylor, L. A. (1989). A negative Ce anomaly in a peridotite xenoliths: Evidence for crustal recycling into the mantle or mantle metasomatism? Geochimica et Cosmochimoca Acta 53: 1035-1040

[40] Nzenti, J. P., Kapajika, B., Worner, G. and Lubala, R. T. (2006). Synkinematic emplacement of granitoids in a Pan-African shear zone in central Cameroon. Journal of African Earth Sciences, 45: 74-86.

[41] Owona, S. (2008). Archaean, Eburnean and Pan-African Features and Relationships in their Junction Zone in the South of Yaounde (Cameroon). PhD Thesis, University of Douala, (232).

[42] Owona, S., Mvondo, J. O., Ekodeck, G. E. (2013). Evidence of quartz, feldspar and amphibole crystal plastic deformation in the Paleoproterozoic Nyong complex shear zones under amphibolites to granulite conditions (West Central African Fold Belt, SW Cameroon). Journal of Geography and Geology, 5(3):186-201.

[43] Owona, S., Schulz, B., Ratschbacher, L., Ondoa, J. M., Ekodeck, G. E., Tchoua, F. M. and Affaton, P. (2011). Pan-African Metamorphism evolution in the southern Yoaunde Group (Qubannguide Complex, Cameroon) as revealed by EMP-Monazite dating and thermobarometry of garnet metapelites. Journal of African Earth Sciences, 59: 125-139.

[44] Pearce, J. A. and Cann, J, R. (1973). Tectonic setting of basic volcanic rocks determined using trace element analyses. Earth and Planetary Science Letters, 19: 290-300.

[45] Pénaye, J., Toteu, S. F., Tchameni, R., Van Schmus, W. R., Tchakounté, J., Ganwa, A., Minyem, D. and Nsifa, E. N. (2004). The 2.1 Ga West Central African Belt in Cameroon: extension and evolution. Journal of African Earth Sciences, 39: 159-164.

[46] Randine, K., Kumar, J. V. and Korakoppa, M. (2015). Platinum-group elements mineralization in the cumulate gabrro of Phenai Mata Complex, Deccan Large Igneous Province, India. Current Science, 108 (10): 1796 - 1798.

[47] Randive, K., Kumar, J. V., Bhondwe, A. and Lanjewar, S. (2014). Understanding the Behaviour of Rare Earth Elements in Minerals and Rocks. Gond. Geol. Mag., V. 29(1 and 2), pp 29-37.

[48] Randive, K.R. (2012). Elements of Geochemistry, Geochemical Exploration and Medical Geology. Research Publishing Services, Singapore, 457p.

[49] Rollinson, H. (1993). Using geochemical data: evaluation, presentation, interpretation. Longman Scientific & Technical, Essex, 352p.

[50] Saleh, G. M. (2007). Geology and rare-earth element geochemistry of highly evolved, molybdenite-bearing granitic plutons, Southeastern Desert Egypt. Chinese Journal of Geochemistry, 26(4): 334-344.

[51] Sun, S. S., Nesbitt, R. W. and Sharaskin, A. Y. (1979). Geochemical Characteristics of Mid-Oceanic Ridge Basalts. Earth and Planetary Science Letters, Vol. 44, pp119-138.

[52] Tack, L., Wingate, M.T.D.,Liégeois, J.P., Fernadez- Alonso, M. and Deblond, A. (2001). Early Neoproterozoic magmatism (1000-910Ma) of the Zadinian and Ma-yumbian Groups (Bas-Congo): Onset of Rodinia rifting at the western edge of the Congo Craton. Precambrian Research, 110: 277-306.

[53] Taylor, S.R. and McLennan, S. M. (1985). The Continental Crust: Its Composition and Evolution. Blackwell, Oxford, 312pp.

[54] Thomas, R. J., Chevallier, L. P., Gresse, P., Harmer, R. E., Eglington, B. M., Armstrong, R. A., DeBeer, C. H., Martini, J. E. J., de Kock, G. S., Macey, P. H. and Ingraham, B.A.(2002). Precambrian evolution of the Sirwa Window, Anti-Atlas Orogen, Morocco. Precambrian Research: 118, 1–57.

[55] Toteu, F. S., Van Schmus, W. R., Penaye, J. and Nyobé, J. B. (1994b).U-Pb and Sm-Nd evidence for Eburnean and Pan-African high grade metamorphism in cratonic rocks of Southern Cameroon. Precambrian Research, 67: 321-347.

[56] Toteu, S. F., Pénaye, J., Van Schmus, W. R. and Michard, A. (1994a). Preliminary U-PB and Sm-Nd geochronologic data on the North Central Cameroon: Contribution of the Archaean and Paleoproterozoic crust to the edification of an active domain of the Pan-African orogeny. Canadian Research of Acadamic Sciences, Paris, 319(Series II): 1519 – 1524.

[57] Verhulst, A., Balaganskaya, E., Kirnarsky, Y., Demaiffe, D. (2000). Petrological and Geochemical ( trace elements and Sr- Nd isotopes) Characteristics of the Paleozoic Kovdor Ultramafic, alkaline and Carbonatite Intrusion 9Kola Peninsula, NW Russia. Lithos, 51, pp1-25.

[58] Vicat, J. P. and Pouclet, A. (2000). Paleo- and Neoproterozoic granitoids and rhyolites from the West Congolian Belt (Gabon, Congo, Cabinda, north Angola): Chemical composition and geotectonic implications. Journal of African Earth Sciences, 31 (3/4): 597 – 617.

[59] Winchester, J. A. and Floyd, P. A. (1976a). Geochemical discrimination of different magma series and their differentiation products using immombile elements. Chemical Geology, 20: 325–343.

[60] Winchester, J. A. and Floyd, P. A. (1976b). Geochemical magma type discrimination: application to altered and metamorphosed basic igneous rocks, Earth and Planetary Science Letters, 28: 459–469.

[61] Winkler, H.G.F. (1976). Petrogenesis of metamorphic rocks. 4th edition, Springer, New York, 334pp.

[62] Winter, J. (2001). Principles of Igneous and Metamorphic Petrology. Second Edition, Pearson Education Limited, Edinburgh Gate, Harlow Essex CM20 2JE, 745pp.

**Citation:** *T. A. Ako, et.al (2018). Trace and Rare Earth Elements Patterns in Metamorphosed Ultramafic Rocks of the Paleoproterozoic Nyong Series, Southeast Cameroon, International Journal of Mining Science (IJMS), 4(4), pp.10-24, DOI: http://dx.doi.org/10.20431/2454-9460.0404002*